

2,2'-Dipyridylamine as Organic Molecular Electrocatalyst for Hydrogen Evolution Reaction in Acidic Electrolytes

Xi Yin, Ling Lin, Hoon T. Chung, Ulises Martinez, Andrew Baker, Sandip Maurya, Piotr Zelenay*

Materials Physics and Application Division, Los Alamos National Laboratory, Los Alamos, New Mexico 87545, USA.

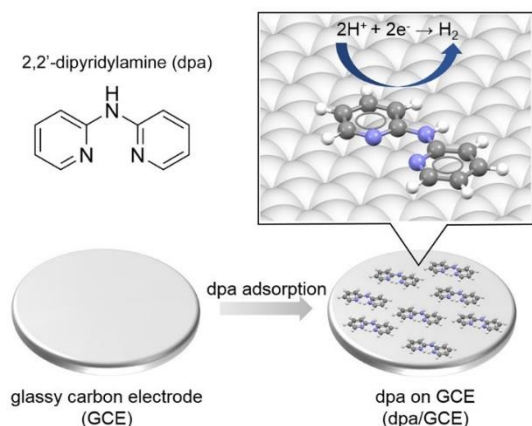
Supporting Information Placeholder

ABSTRACT: Finding a low-cost and stable electrocatalyst for hydrogen evolution reaction (HER) as a replacement for scarce and expensive precious metal catalysts has attracted significant interest from chemical and materials research communities. Here, we demonstrate an organic catalyst based on 2,2'-dipyridylamine (dpa) molecules adsorbed on carbon surface, which shows remarkable hydrogen evolution activity and performance durability in strongly acidic polymer electrolytes without involving any metal. The HER onset potential at dpa adsorbed on carbon has been found to be less than 50 mV in sulfuric acid and in a Nafion[®]-based membrane electrode assembly (MEA). At the same time, this catalyst has shown no performance loss in a 60-hour durability test. The HER reaction mechanisms and the low onset overpotential in this system are revealed based on electrochemical study. Density functional theory (DFT) calculations suggest that the pyridyl-N functions as the active site for H adsorption with a free energy of -0.13 eV, in agreement with the unusually low onset overpotential for an organic molecular catalyst.

Hydrogen evolution reaction (HER) catalysts play vital role in hydrogen economy by facilitating the reduction of protons to the H₂ molecule ($2\text{H}^+ + 2\text{e}^- \rightarrow \text{H}_2$), the reaction of fundamental importance in the production of hydrogen as an ultimate clean fuel.¹⁻⁶ HER catalysts also function as critical components in hydrogen purification/compression systems, operating on the electrochemical “hydrogen pump” principle.⁷⁻⁹ So far, most HER catalysts contain metals in the form of pure metals, alloys, inorganic compounds, metal complexes, or dopants. The possibility of utilizing metal-free organic molecules, with the HER active sites consisting of the most earth-abundant elements such as C, N, H, is highly appealing but at the same time challenging. Early research using a dropping mercury electrode (DME) revealed HER activity of N-containing organic molecules, *e.g.*, albumins and pyridine.¹⁰⁻¹⁴ These molecules can potentially serve as an effective platform for the design of electrocatalysts with many unique advantages, including (a) high elemental abundancy; (b) well-defined and tunable structure; (c) virtually infinite molecular design space; and (d) robust configuration of covalently bonded atoms promising good chemical stability in highly acidic polymer electrolytes. However, these attractive candidate materials often suffer from the HER onset overpotential (η_{onset}) on the order of hundreds of mV, much too high for practical applications.¹¹⁻¹⁸ In most previous studies the use of organic molecules was restricted to enhancing HER activity of metals.^{15,16} Until now, there has been no report on the successful development of organic molecules with a viable HER activity in acidic polymer elec-

trolytes. Herein, we demonstrate an organic molecular electrocatalyst based on 2,2'-dipyridylamine (dpa) supported on carbon (Scheme 1) with an extremely low onset potential of *ca.* 50 mV, high HER activity and excellent durability in acidic media, including an acidic polymer electrolyte.

Scheme 1. 2,2'-Dipyridylamine (dpa) Adsorbed on Carbon as Heterogeneous Electrocatalyst for Hydrogen Evolution Reaction.



The HER activities of dpa adsorbed on a polished glassy carbon electrode (dpa/GCE) and clean glassy carbon electrode (GCE) were evaluated at a rotating disk electrode (RDE) in an electrochemical cell using N₂-saturated 0.5 M H₂SO₄ as a supporting electrolyte. A graphite rod was used as a counter electrode to avoid any possible metal contamination of the molecular catalyst in the working electrode. The current density (*j*) was normalized to the geometric surface area of the GCE. At 80 °C, the GCE-supported dpa exhibits high HER activity, reflected by η_{onset} of *ca.* 0.05 V and *j* of 10 mA/cm² at -0.35 V vs. RHE (Figure 1a). The trace amounts of potentially HER-active transition metals in as-received dpa and GCE were less than 1 ppm (Table SI-SII). This level of concentration, was many orders of magnitude below that in metal-based HER catalysts, *e.g.*, 2.9 - 5.9 10⁴ ppm of nickel in Ni complex-based catalysts^{19,20}, making any HER activity originating from the traces of the transition metals, if at all present, unlikely. The electrochemical experiment described above was conducted using high-purity sulfuric acids of ACS Plus and Optima[®] grades, with transition metal impurity level less than 0.2 ppm, and 10 ppt, respectively. No decrease in HER activity was observed following a decrease in the concentration of trace metals in the acid used (Figure S1-S2), which proves that metal impurities in sulfuric acid at the ppt-to-ppm levels had no effect on HER activity of the dpa catalyst.

At 80 °C, the Tafel slope for HER at dpa/GCE in the linear part of the overpotential (η)- $\log j$ plot is 85 ± 4 mV/dec and the exchange current density is $1.3 \pm 0.3 \cdot 10^{-5}$ A/cm²_{GCE} (Figures 1b and S1). At 25 °C, the two values are 72 ± 3 mV/dec and $6 \pm 2 \cdot 10^{-7}$ A/cm²_{GCE}, respectively (Figure S2). Table SIII summarizes the key activity metrics for dpa/GCE and graphitic carbon nitride (C₃N₄) catalysts, polymer-coated GCE, and homogeneous organic molecules tested on copper or silver electrodes. Low values of both the onset overpotential and Tafel slope attest to high HER activity of dpa/GCE.

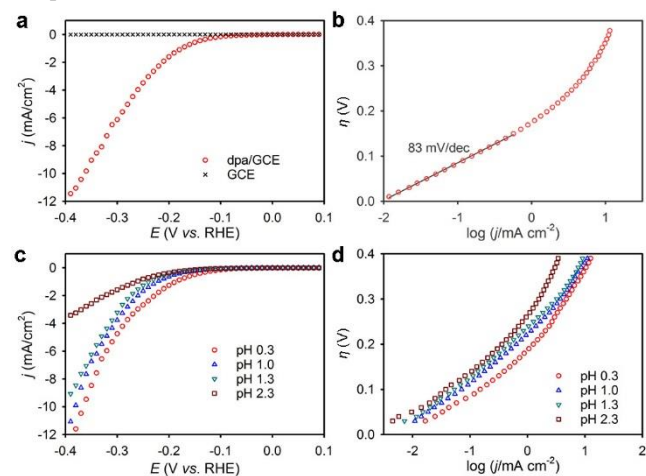


Figure 1. (a) Steady-state HER polarization plots for dpa adsorbed on glassy carbon electrode (dpa/GCE) in N₂-saturated 0.5 M H₂SO₄ at 80 °C. 10 mV steps, 32 s/step. (b) Tafel plot of HER at dpa/GCE in N₂-saturated 0.5 M H₂SO₄ at 80 °C. (c-d) HER polarization plots and Tafel plots for dpa/GCE in N₂-saturated solutions with different pH at 80 °C. 10 mV steps, 32 s/step.

Three HER steps, the Volmer step ($\text{H}_3\text{O}^+ + \text{e}^- + * \rightarrow \text{H}^* + \text{H}_2\text{O}$), the Heyrovsky step ($\text{H}^* + \text{H}_3\text{O}^+ + \text{e}^- \rightarrow \text{H}_2\uparrow$), and the Tafel step ($2\text{H}^* \rightarrow 2* + \text{H}_2\uparrow$), are widely accepted as best describing HER on conventional metal-based catalysts, where H* is the adsorbed H at an active site *. The predicted Tafel slope values associated with these steps are close to 120, 40, and 30 mV/dec, respectively. However, it is challenging to determine the exact mechanism solely based on the Tafel slope due to the complexity of HER kinetics at the dpa/GCE electrode. For dpa/GCE, the Tafel plot is linear in the overpotential range from 0 to 0.15 V (Figure 1b), becoming non-linear at higher overpotentials, with the tangential slope gradually increasing to more than 300 mV/dec. The fact that it far exceeds 120 mV/dec suggests a Tafel-like recombination step of two adsorbed H atoms as the rate-determining step at high overpotentials.^{5,21} Adsorption of H atoms may happen at the pyridyl-N sites, as suggested by previous research involving heterocycle molecules.^{11,13,14}

Figure 1c depicts the dependence of the dpa/GCE HER activity on electrolyte pH. The order of reaction with respect to proton concentration, $p_{(\text{H}^+)}$, was determined to be *ca.* 0.3 (Figure S3). This fractional number implies a multi-step mechanism and possibly multiple reaction pathways.²² It was previously suggested that $p_{(\text{H}^+)}$ can be less than one when the Tafel step is rate determining.²² At overpotentials lower than 200 mV, an increase in the pH from 0.3 to 2.3 results in an increase in the Tafel slope from *ca.* 90 to *ca.* 105 mV/dec (Figure 1d). At overpotentials greater than 200 mV, the Tafel dependence is no longer linear. The tangential slope values increase from *ca.* 200 mV/dec to *ca.* 270 mV/dec upon an increase in pH from 0.3 to 2.3. These results attest to a change in the HER kinetics with a change in pH.²²

In order to understand the role of pyridyl-N and amine group in the HER activity, we screened several dpa analogs for their HER

activity (Figure 2a). All studied molecules had the pyridyl and amine groups but in different configurations. Under the same test conditions, none of the molecules adsorbed on GCE showed HER activity comparable to that of dpa/GCE (Figures 2b and S4), suggesting that the mere presence of the pyridyl and amine groups does not guarantee high HER activity.

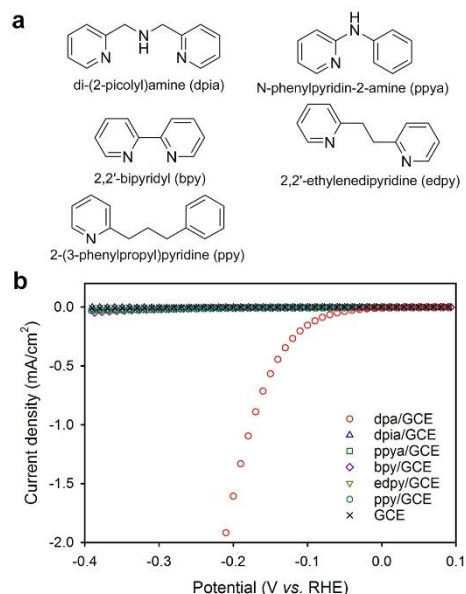


Figure 2. HER activity comparison for dpa and its analogs adsorbed on glassy carbon electrode in N₂-saturated 0.5 M H₂SO₄ at 80 °C. 10 mV steps, 32 s/step.

Fourier transform infrared spectroscopy (FT-IR) analysis was carried out to gain insight into the state of protonated dpa in acidic media, which is likely to get involved in the HER process.^{11,13,14} The results show that, depending on pH, the dpa molecules can be in either mono- or di-protonated state, as reflected by characteristic features in the IR spectra (Figures S5-S6). A detailed discussion of the interaction of dpa with acidic media is included in the Supporting Information.

The HER activity of dpa supported on high surface-area carbon (dpa/C) was further demonstrated in a polymer membrane electrode assembly (MEA). Figure 3a depicts HER performance of the dpa/C catalyst in a Nafion[®]-based MEA tested in the H₂-pump mode of operation,⁹ with dpa/C and Pt/C acting as the cathode and anode catalyst, respectively (Figure S7). H₂ was flown through both anode and cathode at the same flow rate and pressure to equalize the chemical potential of H₂ on both sides of the cell.⁹ A bias voltage was applied so that HER took place at the dpa/C cathode and hydrogen oxidation reaction (HOR) occurred at the Pt/C anode. At 80 °C, the onset potential of hydrogen evolution was *ca.* -0.05 V vs. RHE, and a current density of 10 mA/cm² was reached at a potential of -0.12 V vs. RHE. (Potential values were corrected for the ohmic loss and polarization loss at Pt/H₂ reference electrode as illustrated in Figure S8, following the approach described in literature.⁹) At 30 °C, the onset potential decreased slightly to *ca.* -0.07 V, and current density of 10 mA/cm² was reached at -0.19 V. Unlike Pt, which is active in both HER and HOR, the dpa/C catalyst is HER-specific. The catalyst exhibits very good durability, as shown by the chronoamperometric data recorded at a constant bias voltage of -0.2 V, with no measurable activity loss over 60 hours (Figure 2b). We also conducted an experiment by flowing H₂ only over the Pt/C anode and collecting H₂ generated at the dpa/C cathode. Based on the volume of collected H₂, the faradaic efficiency of the HER was 99% ± 2%.

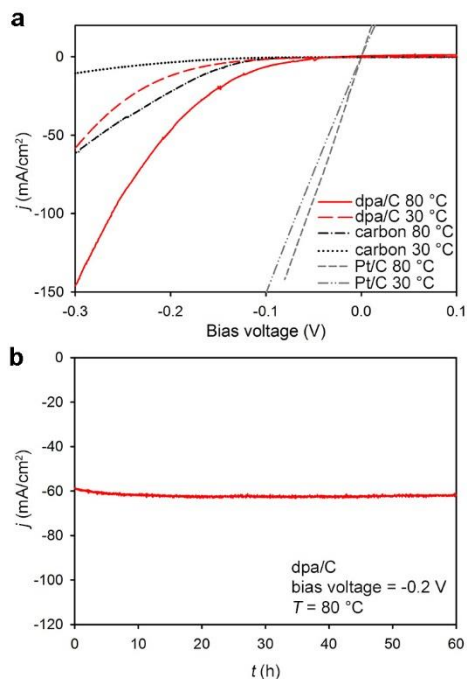


Figure 3. HER performance of dpa/C in MEA test. (a) Polarization plots of 5 cm² MEAs in H₂-pump experiment at 80 °C and 30 °C. Cathode: dpa/C 3 mg/cm², 30 wt% dpa; carbon black 2 mg/cm² or Pt 0.03 mg/cm²; 200 sccm H₂, ambient pressure; anode: Pt 0.3 mg/cm²; 200 sccm H₂, ambient pressure; membrane: two layers of Nafion[®] NRE-212; scan rate: 1 mV/s. (b) Durability test of the dpa/C cathode during HER at a -0.20 V bias voltage.

We conducted density functional theory (DFT) calculations to understand mechanism behind the very low HER onset overpotential and high activity of dpa. The HER process heterogeneously catalyzed by dpa adsorbed on carbon support was studied using computational hydrogen electrode (CHE) approach.²³ In this approach, the adsorption energy of hydrogen atom at the active site (ΔG_{H}) has been proven to be a suitable activity descriptor for a broad range of HER catalysts, including both metal-based and metal-free materials.^{5,24,25} By the Sabatier principle, the binding of atomic H to an effective HER catalyst should neither be too strong nor too weak. Consequently, smaller $|\Delta G_{\text{H}}|$ values represent lower thermodynamic barrier for the HER. In an ideal case, ΔG_{H} is expected to be 0 eV. We first modeled dpa adsorbed on the graphite (0001) surface (dpa/graphite) under periodic boundary conditions (**Figure S9**). We then assumed that the intermediate state involved H atom bound to one of the pyridyl-N sites in the dpa molecule adsorbed on graphite (**Figures 3a-b**). We calculated ΔG_{H} based on the change in the total energy (**Table SIV**), with corrections for the change in zero point energy and vibrational entropy of the system. The ΔG_{H} for dpa/graphite model was found to be -0.13 eV, close to -0.09 eV for Pt(111) surface model and 0 eV for the ideal HER catalyst.²³ The $|\Delta G_{\text{H}}|$ of 0.13 eV represents a low thermodynamic barrier for HER on the dpa/graphite catalyst (**Figure 3c**), agreeing well with the low experimental HER onset overpotential of 0.05 V. Incidentally, this thermodynamic barrier is also lower than those predicted from metal-free catalyst models of graphitic-carbon nitride carbon nitride (g-C₃N₄), nitrogen-doped graphene (N-graphene; NG), and g-C₃N₄ on N-graphene (C₃N₄@NG).⁵

We used DFT calculation to assess the likelihood of HER to occur at dpa by a homogeneous catalysis mechanism. Several homogeneous HER pathways involving dpa and its various states in solution were studied (**Figure S10-20**, **Table SV**, see details in Supporting Information). However, the predicted HER potential values were much lower than those obtained using the surface model. The differences between potential values in the two cases suggest that

the interaction of adsorbed dpa molecule with the carbon substrate may play an essential role in lowering the thermodynamic energy barrier for the HER.

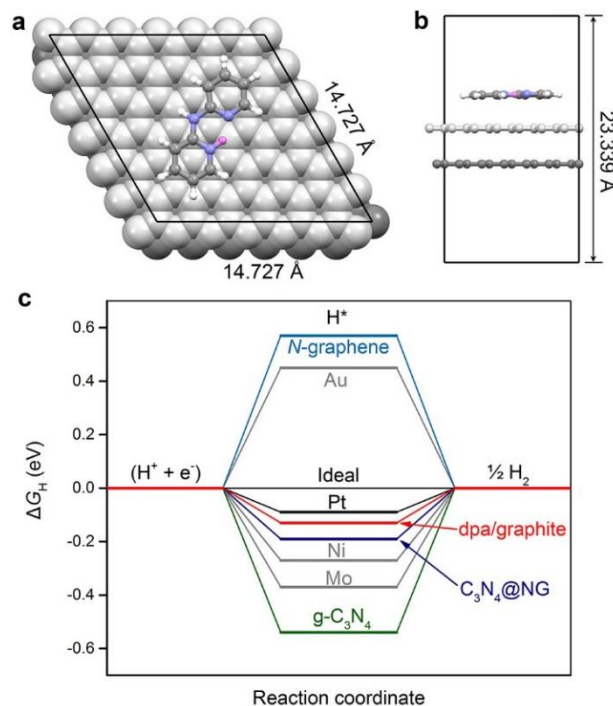


Figure 4. Atomic H bond to the pyridyl-N site of dpa adsorbed on graphite (0001) surface: (a) top view, (b) side view. Colors: N – blue, C – grey, H – white. The top and bottom layers of the (0001) plane of graphite are in light grey and dark grey, respectively. The adsorbed atomic H is shown in pink. (c) Adsorption energy of hydrogen atom, ΔG_{H} , on the dpa/graphite catalyst and on other model catalysts. Data retrieved from references.^{5,23}

In summary, we demonstrate here a unique organic HER catalyst based on 2,2'-dipyridylamine (dpa). The onset potential for hydrogen evolution at this metal-free catalyst in an acidic electrolyte is *ca.* 50 mV, a very low value for any HER catalyst. The dpa catalyst also showed high HER activity and excellent stability over for 60 hours of operation in the polymer electrolyte, fully compatible with the established proton exchange membrane (PEM) technology. The electrochemical study revealed a complex HER mechanism for the dpa-on-carbon system, with Tafel step being rate-determining at high overpotentials. DFT study allowed to correlate high HER activity of the dpa catalyst with adsorption energy of atomic hydrogen on pyridyl-nitrogen in dpa molecule on graphite. The discovery of HER activity of dpa potentially paves the way for designing new high-performance, low-cost, sustainable electrocatalysts based on metal-free organic molecules.

ASSOCIATED CONTENT

Supporting Information

The Supporting Information is available free of charge on the ACS Publications website. Materials and methods, Tafel plots of multiple HER polarization curves, description of electrochemical hydrogen pump experiments, FTIR spectra of dpa in acids, DFT calculation results using homogeneous solution model and surface model (PDF)

AUTHOR INFORMATION

Corresponding Author

*E-mail: zelenay@lanl.gov

Notes

A provisional patent application has been filed based on this research work.

ACKNOWLEDGMENT

The authors would like to thank Edward Holby, Yu Seung Kim, Eric Brosha, and Gerie Purdy for helpful discussion and assistance in with experiments. We also thank Hong Yang and Jaemin Kim at the University of Illinois Urbana-Champaign for performing ICP-MS experiments. Financial support for this research by Los Alamos National Laboratory through Laboratory Directed Research and Development (LDRD) is gratefully acknowledged. We also thank the DOE-EERE Fuel Cell Technologies Office (FCTO) for continuous support of Los Alamos energy research.

REFERENCES

- (1) Seh, Z. W.; Kibsgaard, J.; Dickens, C. F.; Chorkendorff, I.; Nørskov, J. K.; Jaramillo, T. F. Combining Theory and Experiment in Electrocatalysis: Insights into Materials Design. *Science* **2017**, *355*, eaad4998.
- (2) Stamenkovic, V. R.; Strmcnik, D.; Lopes, P. P.; Markovic, N. M. Energy and Fuels from Electrochemical Interfaces. *Nat. Mater.* **2017**, *16*, 57.
- (3) Roger, I.; Shipman, M. A.; Symes, M. D. Earth-Abundant Catalysts for Electrochemical and Photoelectrochemical Water Splitting. *Nat. Rev. Chem.* **2017**, *1*, 0003.
- (4) Ambrosi, A.; Chua, C. K.; Latiff, N. M.; Loo, A. H.; Wong, C. H. A.; Eng, A. Y. S.; Bonanni, A.; Pumera, M. Graphene and Its Electrochemistry - An Update. *Chem. Soc. Rev.* **2016**, *45*, 2458.
- (5) Zheng, Y.; Jiao, Y.; Zhu, Y.; Li, L. H.; Han, Y.; Chen, Y.; Du, A.; Jaroniec, M.; Qiao, S. Z. Hydrogen Evolution by a Metal-Free Electrocatalyst. *Nat. Comm.* **2014**, *5*, 3783.
- (6) Dai, L.; Xue, Y.; Qu, L.; Choi, H.-J.; Baek, J.-B. "Metal-Free Catalysts for Oxygen Reduction Reaction". *Chem. Rev.* **2015**, *115*, 4823.
- (7) Fishel, K.; Qian, G.; Eisman, G.; Benicewicz, B. C. Electrochemical Hydrogen Pumping. In *High Temperature Polymer Electrolyte Membrane Fuel Cells: Approaches, Status, and Perspectives*; Li, Q., Aili, D., Hjuler, H. A., Jensen, J. O., Eds.; Springer International Publishing: Cham, 2016, p 527.
- (8) Ströbel, R.; Oszcipok, M.; Fasil, M.; Rohland, B.; Jörissen, L.; Garcke, J. The Compression of Hydrogen in an Electrochemical Cell Based on a PE Fuel Cell Design. *J. Power Sources* **2002**, *105*, 208.
- (9) Neyerlin, K. C.; Gu, W.; Jorne, J.; Gasteiger, H. A. Study of the Exchange Current Density for the Hydrogen Oxidation and Evolution Reactions. *J. Electrochem. Soc.* **2007**, *154*, B631.
- (10) Heyrovský, J.; Babička, J. Polarographic Studies with the Dropping Mercury Kathode. Part XIII. The Effect of Albumins. *Collect. Czech. Chem. Commun.* **1930**, *2*, 370.
- (11) Mairanovskii, S. G. The Theory of Catalytic Hydrogen Waves in Organic Polarography. *J. Electroanal. Chem.* **1963**, *6*, 77.
- (12) Stradyn', Y. P.; Kadysh, V. P.; Giller, S. A. Polarography of Heterocyclic Compounds. *Chem. Heterocycl. Com.* **1973**, *9*, 1435.
- (13) Heyrovský, M. Catalytic Hydrogen Evolution at Mercury Electrodes from Solutions of Peptides and Proteins. In *Perspectives in Bioanalysis*; Emil Paleček, F. S., Wang, J., Eds.; Elsevier: 2005; Vol. Volume 1, p 657.
- (14) Leibson, V. N.; Churilina, A. P.; Mendkovich, A. S.; Gulyai, V. P. New Ideas of the Mechanism of Catalytic Hydrogen Evolution in the Buffer Solutions of Organic Compounds. *J. Electroanal. Chem. Interfacial Electrochem.* **1989**, *261*, 165.
- (15) Váduva, C. C.; Vaszilcsin, N.; Kellenberger, A. Aromatic Amines as Proton Carriers for Catalytic Enhancement of Hydrogen Evolution Reaction on Copper in Acid Solutions. *Int. J. Hydrogen Energy* **2012**, *37*, 12089.
- (16) Uchida, T.; Mogami, H.; Yamakata, A.; Sasaki, Y.; Osawa, M. Hydrogen Evolution Reaction Catalyzed by Proton-Coupled Redox Cycle of 4,4'-Bipyridine Monolayer Adsorbed on Silver Electrodes. *J. Am. Chem. Soc.* **2008**, *130*, 10862.
- (17) Liu, L.; Zha, D.-W.; Wang, Y.; He, J.-B. A Nitrogen- and Sulfur-Rich Conductive Polymer for Electrocatalytic Evolution of Hydrogen in Acidic Electrolytes. *Int. J. Hydrogen Energy* **2014**, *39*, 14712.
- (18) Kurys, Y. I.; Mazur, D. O.; Koshechko, V. G.; Pokhodenko, V. D. Electrocatalysis of Electrochemical Hydrogen Evolution from Water in Acid Media using N-Containing Conjugated Polymers. *Theor. Exp. Chem.* **2016**, *52*, 163.
- (19) Helm, M. L.; Stewart, M. P.; Bullock, R. M.; DuBois, M. R.; DuBois, D. L. A Synthetic Nickel Electrocatalyst with a Turnover Frequency above 100,000 s⁻¹ for H₂ Production. *Science* **2011**, *333*, 863.
- (20) Le Goff, A.; Artero, V.; Josselme, B.; Tran, P. D.; Guillet, N.; Métayé, R.; Fihri, A.; Palacin, S.; Fontecave, M. From Hydrogenases to Noble Metal-Free Catalytic Nanomaterials for H₂ Production and Uptake. *Science* **2009**, *326*, 1384.
- (21) Shinagawa, T.; Garcia-Esparza, A. T.; Takanabe, K. Insight on Tafel Slopes from a Microkinetic Analysis of Aqueous Electrocatalysis for Energy Conversion. *Sci. Rep.* **2015**, *5*, 13801.
- (22) Kahyarian, A.; Brown, B.; Nescic, S. Mechanism of the Hydrogen Evolution Reaction in Mildly Acidic Environments on Gold. *J. Electrochem. Soc.* **2017**, *164*, H365.
- (23) Nørskov, J. K.; Bligaard, T.; Logadottir, A.; Kitchin, J. R.; Chen, J. G.; Pandelov, S.; Stimming, U. Trends in the Exchange Current for Hydrogen Evolution. *J. Electrochem. Soc.* **2005**, *152*, J23.
- (24) Zheng, Y.; Jiao, Y.; Li, L. H.; Xing, T.; Chen, Y.; Jaroniec, M.; Qiao, S. Z. Toward Design of Synergistically Active Carbon-Based Catalysts for Electrocatalytic Hydrogen Evolution. *ACS Nano* **2014**, *8*, 5290.
- (25) Nørskov, J. K.; Bligaard, T.; Rossmeisl, J.; Christensen, C. H. Towards the Computational Design of Solid Catalysts. *Nat. Chem.* **2009**, *1*, 37.

Table of Contents (TOC)

